

Cumulative instabilities of the nonthermal solar wind electrons: strahls (heat fluxes), temperature anisotropies and suprathermals

S.M.Shaaban^{1,2,3}, M. Lazar^{1,2}, S. Poedts²

¹ *Centre for Mathematical Plasma Astrophysics, KU Leuven, Leuven, Belgium*

² *ITP IV, Weltraum- und Astrophysik, Ruhr-Universität Bochum, Bochum, Germany*

³ *Theoretical Physics Research Group, Faculty of Sci., Mansoura University, Mansoura, Egypt*

Abstract

The velocity distributions of solar wind electrons reveal two central components, a low-energy thermal core and a suprathermal population incorporating both the halo and strahl components, which are responsible for the electron heat-flux in space plasmas. Hotter and more dilute, suprathermal electrons may also exhibit (intrinsic) temperature anisotropies, especially with respect to the magnetic field direction. In the existing studies these sources of free energy and the resulting instabilities are investigated independent of each other. Here we revisit the critical conditions of these instabilities, and provide new insights from their interplay. Regimes of instability are accurately delimited establishing their nature, although distinguishing between them becomes highly demanding.

1. Introduction

The in-situ measurements of the solar wind electron velocity distributions (eVDs) at different heliocentric distances reveal strong deviations from a simple Maxwellian model. The observed eVDs exhibit three components: a Maxwellian (thermal) core, a suprathermal halo, and a drifting field aligned component, also known as strahl [1]. Both core and halo components can be anisotropic, with $A = T_{\perp}/T_{\parallel} \neq 1$ (where \perp and \parallel denote the perpendicular and parallel directions to the background magnetic field, respectively) [2]. Strahls are generally observed in the fast winds, and here we consider a combined halo-strahl scenario, in which both the drifting strahl and halo components are effectively included in the beam population. Shaaban et al. (2018)[3] show that depending on the beaming velocity, two distinct branches can be destabilized: The right-handed (RH) whistler heat-flux instability (WHFI) if beaming velocity is lower than thermal speed, and the firehose heat-flux instability (FHFI) with a left-handed (LH) polarization and driven by more energetic beams. These instabilities have dispersive characteristics similar to the whistler (WI) driven by a temperature anisotropy $A > 1$, and electron firehose instabilities (EFH) driven by $A < 1$. Theoretical attempts to characterize the heat-flux and anisotropy driven instabilities have completely ignored the cumulative effects of the two sources of free

energies [3, 4, 5]. Here we show that the interplay of beaming electrons and their temperature anisotropies can markedly change linear dispersive properties of the heat-flux instabilities.

2. Dispersion relations

We consider the eVDF with a dual structure, combining a beam (subscript b) and a core (subscript c), counterstreaming in a frame fixed to protons [3]

$$F_e(v_\perp, v_\parallel) = \delta f_b(v_\perp, v_\parallel) + (1 - \delta) f_c(v_\perp, v_\parallel), \quad (1)$$

where $\delta = n_b/n_0$ is the relative beam density, and n_0 is the electron total number density.

These two components may be anisotropic, assuming a drifting bi-Maxwellian core and a drifting bi-kappa distributed beam. The drifting velocities U_c and U_b for the core and beam components, respectively, are directed along the background magnetic field and satisfy a zero net current condition, $n_b U_b = n_c U_c$, in a quasi-neutral electron-proton plasma, $n_e = n_c + n_b \approx n_p$.

For thermal isotropic protons, the general dispersion relations for the parallel ($\mathbf{k} \parallel \mathbf{B}$) electromagnetic (EM) waves read [8]

$$K^2 = \frac{1}{\eta} \left[A_c - 1 + \frac{A_c (\tilde{w} + u_c K) \mp (A_c - 1)}{K \sqrt{\beta_c}} Z \left(\frac{W \mp 1 + u_c K}{K \sqrt{\beta_c}} \right) \right] + \frac{W}{\delta K \sqrt{\mu \beta_p}} Z \left(\frac{\mu W \pm 1}{K \sqrt{\mu \beta_p}} \right) + A_b - 1 + \frac{A_b (W - u_b K) \mp (A_b - 1)}{K \sqrt{\beta_b}} Z_K \left(\frac{W \mp 1 - u_b K}{K \sqrt{\beta_b}} \right) \quad (2)$$

where $K = c k / \omega_{p,e}$, $W = \omega / |\Omega_e|$, $\eta = (1 - \delta) / \delta$ is the core-beam density contrast, $\mu = m_p/m_e$ is the proton-electron mass contrast, $\beta_a = 8\pi n_a k_B T_{a,\parallel} / \mathbf{B}^2$ is the plasma beta for the population of sort a , \pm denotes the circular right-handed (RH) and left-handed (LH) polarizations, respectively, $u_b = U_b \omega_{p,e} / (c \Omega_e)$ and $u_c = \delta u_b / (1 - \delta)$ are the relative velocities of the beam and core components, respectively, $A_b = T_{b,\perp} / T_{b,\parallel}$, $A_c = T_{c,\perp} / T_{c,\parallel}$ are the beam and core temperature anisotropy, $\xi_a = (\omega - kU_a) / \alpha_{a,\parallel}$, and $Z(\xi_a^\pm)$ is the plasma dispersion function [6] of argument $\xi_a^\pm = (\omega \pm \Omega_a - kU_a) / k\alpha_{a,\parallel}$ and $Z_K(\xi_a^\pm)$ is the modified (Kappa) dispersion function [7] of argument of argument $\xi_b^\pm = (\omega \pm \Omega_e + kU_b) / k\theta_\parallel$.

3. Results

As already mentioned, two modes can be destabilized, e.g., WHF and FHF modes, as a function of the beam-core drift velocity u_b . Therefore, only the instability thresholds can offer a clear and comprehensive picture for the existence and dominance regime of these modes. Here, thresholds are derived for maximum growth rates $\gamma_m / |\Omega_e| \approx 10^{-4}$, and are obtained with an inverse correlation law between the beaming velocity u_b and core plasma beta β_c as $u_b = (1 + a/\beta_c^b) c/\beta_c^d$, where a, b, c, d are the fitting parameters, tabulated in Refs.[3, 8].

For isotropic core-beam scenario, the growth rates of the WHFI exhibit a non-uniform variation, increasing and then decreasing as u_b increases, and therefore, the unstable regimes for WHFI is bounded by two, upper and lower thresholds, as shown in panels (a) and (b) of Fig. 1. The same panels illustrate the effect of the beam suprathermal population on the WHFI thresholds: the upper threshold is increased, while the lower threshold is decreased with increasing the suprathermal populations, i.e., lowering κ . The sum of these effects makes unstable regime of the WHF modes to expand.

The variations of the FHFI thresholds as a function of the core plasma beta and beam power-index κ resemble those variations of the WHF upper threshold, but the unstable FHF regime is located above the thresholds, as indicated by blue arrows in panels (c) and (d). Therefore, it is reasonable to perform a comparison only between the FHFI thresholds and the upper WHFI thresholds. This comparison is provided in panel (c) and (d) for $\kappa \rightarrow \infty$ and $\kappa = 3$, respectively. Panel (c) show clearly the FHF modes are stable for $u_b < 2.5$ and WHF instability is dominant. For higher beam velocities $u_b > 2.7$ and sufficiently large core plasma beta $\beta_c > 0.5$ both WHF and FHF instabilities may coexist, see gray area between their thresholds. This interplay regime further expands as the power index decreases, i.e., for $\kappa = 3$, in panel (d).

In Figure 2 we present the effect of the anisotropic beams on the interplay regime, where FHFI and WHFI may co-exist. We consider bi-Maxwellian distributed beam in order to isolate the effects of the beam anisotropy on the beaming velocity thresholds. In panel (a) the beam anisotropy $A_e = 0.7$ has an inhibiting effect on both the FHFI and WHFI thresholds and determine the interplay regime to move towards lower $u_b > 3.17$ and higher $\beta_c > 0.78$. For an opposite anisotropy $A_b = 1.5$, the beam has a stimulating effect on the beaming velocity thresholds for both FHFI and WHFI and makes the interplay regime to move towards higher $u_b = 3.45$ and higher $\beta_c > 0.5$. For completeness, in panel (c) we show that the lower WHFI threshold markedly decreases even

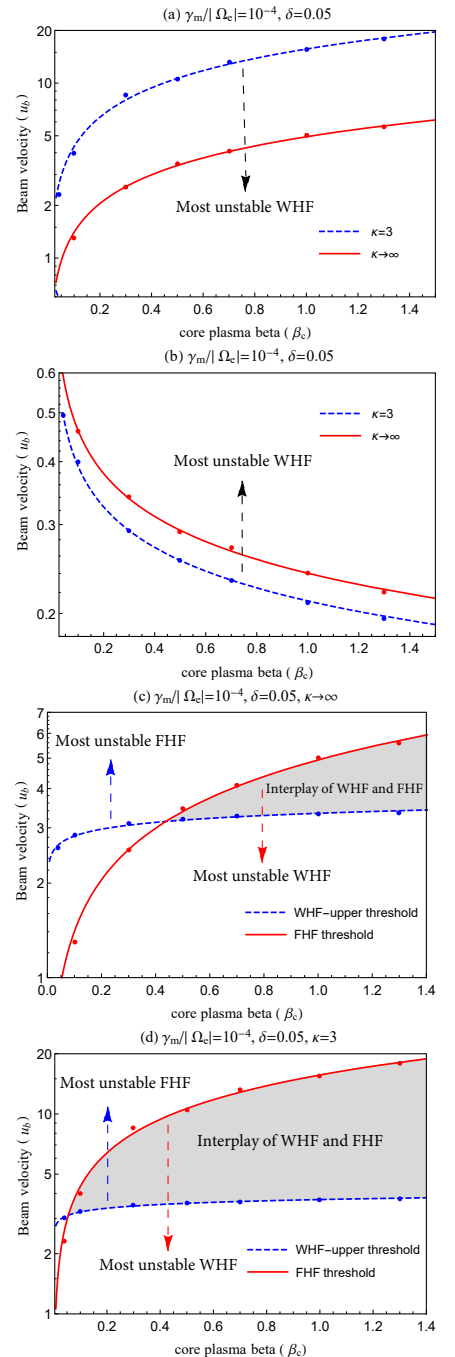


Figure 1: Beaming velocity thresholds for WHFI (a,b) and a comparsion between the FHFI and WHFI thresholds (c,d) (after Ref.[3])

for a relatively small temperature anisotropy $A_b = 1.1$ of the beam, leading to a new unstable regime in which both WI and WHFI can co-exist and interplay.

4. Conclusions

We present a refined analysis of the electron heat flux instabilities by considering the interplay of the beaming electrons and their suprathermal populations as well as their anisotropies, which can markedly change their dispersive characteristics. Thus, we have identified new unstable regimes, where both WHFI and FHF can co-exist and compete. These interplay regimes are found to be very sensitive to the abundance of the beam suprathermal population, i.e., increasing with decreasing κ , see Fig. 1 (c) and (d). Moreover, boundaries of these regimes and are determined by u_b and β_c , are markedly altered with changing the temperature anisotropy, as we have shown in Fig. 2 (a) and (b). In Fig. 2 (c) we have described the effect of the beam anisotropy $A_b > 1$ on the lower WHFI threshold, which decreases by a relatively small anisotropy $A_b = 1.1$. However, this anisotropy is sufficient to excite WI with significant growth rates, if the core plasma beta is large enough $\beta_c > 0.4$ and in this case both WI and WHFI can co-exist and interplay, see the area below the red threshold. Finally, we can conclude that a proper modeling of the velocity distributions in accord to the observations can provide more realistic results and uncover new unstable regimes, which need to be taken into account.

References

- [1] Pierrard, V., Maksimovic M., and Lemaire, J. (1999), JGR, 104.A8, 17021.
- [2] Štverák, Š., et al. (2008), JGR, 113.A3.
- [3] Shaaban S. M., Lazar, M., Poedts, S. (2018), MNRAS, doi.org/10.1093/mnras/sty1567 Ref.[8])
- [4] Gary, S. P. (1985), JGR, 90(A11), 10815
- [5] Lazar, M., Shaaban, S. M., Fichtner, H. and Poedts, S. (2018), PoP, 25(2), 022902.
- [6] Fried, B. and Conte, S. (1961), New York: Academic Press
- [7] Lazar, M., R. Schlickeiser, and P. K. Shukla. Physics of plasmas 15.4 (2008): 042103.
- [8] Shaaban, s. M., Lazar, M., Yoon, P. H., Poedts, S., PoP, under review

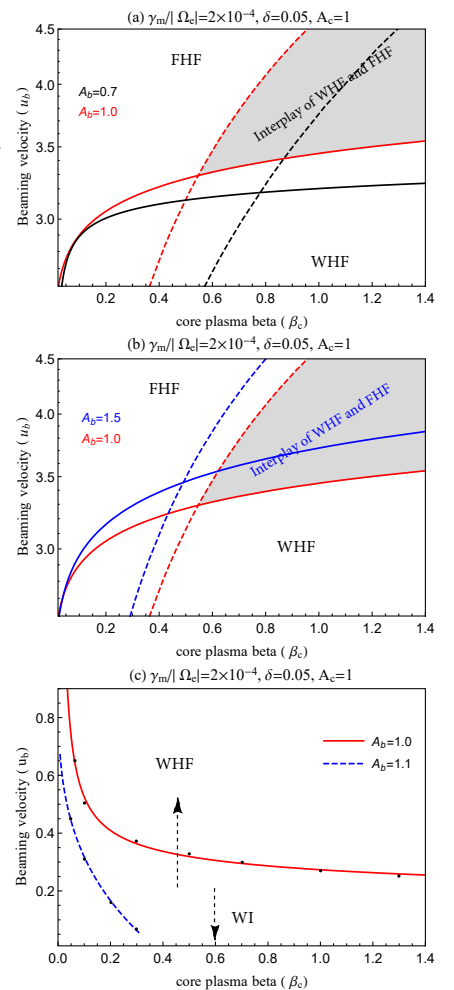


Figure 2: Effects of beam anisotropies on the HF instability thresholds (after